Electron-beam confinement by rotational stabilization in a linear wiggler free electron laser

L. Friedland[a] and R. E. Shefer
Science Research Laboratory, Inc., Somerville, Massachusetts 02143

(Received 1 March 1990; accepted for publication 24 July 1990)

Finite radius electron-beam transport in a linear wiggler free-electron laser with a guide magnetic field is investigated. The addition of a guide magnetic field improves the beam confinement, but also leads to a detrimental drift in the direction transverse to the wiggler magnetic field. The introduction of a rotational transformation of the wiggler magnetic field is proposed to further improve the beam confinement. It is shown that the transformation results in a stable, uniform, solid body rotation of the beam provided (a) the guide field is larger than the amplitude of the wiggler field, (b) the electron drift velocity is much smaller than the rotation speed of the wiggler field as seen by the beam, and (c) the wiggler field rotates in the direction opposite to the direction of the electron gyromotion in the guide field. Theoretical predictions of the improvement of the radial beam transport with the introduction of the rotation of the wiggler field are confirmed in numerical simulations.

I. INTRODUCTION

Linear wigglers based on permanent rare-earth cobalt magnets[1] are now widely used in free-electron lasers (FELs).[2] Among the numerous advantages of using the permanent magnet technology in constructing wigglers for FELs are engineering simplicity, large field amplitude on the axis, adjustability, and ease of access to the beam line. There exists, however, a serious disadvantage of linear wigglers for FEL applications, i.e., the poor beam stability in the direction transverse to the wiggler magnetic field. The problem of beam transport becomes especially important in collective, low-γ FELs.

Conventionally, quadrupole magnetic fields are added to the linear wiggler for stabilization,[3] complicating the configuration significantly. Alternatively, the use of curved[4] or canted[5] poles and the addition of a guide magnetic field[6] have been investigated. Canted magnets introduce focusing in the transverse direction, but, like quadrupoles lead to slow betatron oscillations in the transverse plane. Focusing without the introduction of betatron oscillations may be obtained using curved pole faces. However, this technique is very difficult to implement in a pure permanent magnet design. A sufficiently strong guide field may also improve the transport, but leads at the same time to transverse drifts of off-axis electrons.[6]

In the present work a new stabilization scheme is proposed, i.e., the *rotation* of the direction of polarization of the wiggler magnetic field in the *presence* of a guide magnetic field. Under certain conditions this technique yields a solid body rotation of the electron beam, thus preserving the circular beam cross section along the length of the wiggler. In Sec. II, the finite radius beam dynamics in the combined linear wiggler and guide magnetic fields is considered. The transverse electron drift is described by using an averaging technique. Slow time-scale equations of motion derived in Sec. II are generalized in Sec. III to describe beam transport with the addition of a slow rotation of the direction of polarization of the wiggler field. Parameter regimes corresponding to stable beam propagation are investigated in Sec. III using these slow time-scale equations. Finally, the results of the calculations are summarized in Sec. IV. Numerical simulations are employed throughout the paper in order to both check the predictions of the analytic theory and to add such important effects as a finite emittance and self-space-charge fields.

II. BEAM DYNAMICS IN CROSSED LINEAR WIGGLER AND GUIDE MAGNETIC FIELDS

Consider a finite radius relativistic electron beam propagating along the axis of combined linear wiggler and guide magnetic fields given by

$$\mathbf{B}=F(z)B_{\perp}\cos(k_0z)\cosh(k_0y)\,\hat{e}_y + [B_{\parallel}-F(z)B_{\perp}\sin(k_0z)\sinh(k_0y)]\,\hat{e}_z, \quad (1)$$

where k_0 is the wiggler wave number, the magnitude of the guide field $B_{\parallel}$ is a constant, and the transition function $F(z)$ describes the adiabatic tapering of the wiggler field amplitude, $\mathbf{B}_{\perp}$, at the entrance. In the following, we shall use

$$F(z)=[1+\exp(-z/L)]^{-1}, \quad (2)$$

where L is the adiabatic transition scale length ($L\gg 2\pi/k_0$).

Neglecting, at this stage, the self-fields of the electron beam, we write the momentum equations describing the individual electrons orbits as

[a]Permanent address: Center for Plasma Physics, Racah Institute of Physics, Hebrew University, Jerusalem, Israel.

 0021-8979/90/224958-06$03.00

$$\dot{u}_x = -u_y\left(\frac{\Omega_\parallel}{\gamma} - \frac{\Omega_\perp}{\gamma}F\sinh(k_0y)\sin(k_0z)\right) + u_z\frac{\Omega_\perp F}{\gamma}\cosh(k_0y)\sin(k_0z)\,,$$

$$\dot{u}_y = u_x\left(\frac{\Omega_\parallel}{\gamma} - \frac{\Omega_\perp F}{\gamma}\sinh(k_0y)\sin(k_0z)\right)\,, \tag{3}$$

$$\dot{u}_z = -u_x\frac{\Omega_\perp F}{\gamma}\cosh(k_0y)\cos(k_0z)\,,$$

where $\mathbf{u} = \mathbf{v}/c$ is the electron velocity normalized to the speed of light, $(\cdots)^{\cdot} = d(\cdots)/d\tau$, $\tau = ct$, and $\Omega_{\perp,\parallel} = eB_{\perp,\parallel}/mc^2$. Note that this definition of the cyclotron frequency $\Omega_{\perp,\parallel}$ differs from the conventional one by a factor of $1/c$, and thus $\Omega_{\perp,\parallel}$ has dimensions of cm^{-1}. We now assume the existence of two different spatial scales, i.e., the *short* spatial scale L_s defined by the wiggler period: $L_s \equiv \lambda_w = 2\pi/k_0$ and the *long* spatial scale

$$L_1 = \min\left(L, \frac{2\pi\gamma}{\Omega_\perp}, \frac{2\pi\gamma}{\Omega_\parallel}\right)\,, \tag{4}$$

such that

$$L_s/L_1 \equiv \delta \ll 1\,. \tag{5}$$

Since the transition scale length L is much longer than L_s by definition, Eq. (5) implies that the beam must be sufficiently relativistic such that,

$$k_0\gamma \gg \max(\Omega_\perp, \Omega_\parallel)\,. \tag{6}$$

Equation (3) may be expanded in the small parameter δ [see Eq. (5)] to obtain solutions of the form

$$u_x = u_{xs} + w_x\cosh(k_0y)\sin(k_0z) + O(\delta^2)\,,$$
$$u_y = u_{ys} + w_y\cosh(k_0y)\cos(k_0z) + O(\delta^3)\,, \tag{7}$$
$$u_z = u_{zs} + O(\delta^2)\,,$$

where u_{xs}, u_{ys}, u_{zs}, w_x, w_y, and y are *slowly* varying quantities in the sense that if A is one of these quantities then

$$L_s\left|\frac{1}{A}\frac{dA}{d\tau}\right| \sim O(\delta)\,. \tag{8}$$

We also assume that

$$w_x \sim O(\delta)\,,\quad w_y \sim O(\delta^2)\,,\quad u_{xs} \sim O(\delta)\,,$$
$$u_{ys} \sim O(\delta^2)\,,\quad u_{zs} \sim O(1)\,. \tag{9}$$

This ordering assumption will be tested *a posteriori* for consistency. By substituting Eqs. (7) into Eqs. (3), keeping the lowest significant order, and averaging over the short spatial scale, we get

$$\dot{u}_{xs} = -u_{ys}\frac{\Omega_\parallel}{\gamma}\,,$$

$$\dot{u}_{ys} = u_{xs}\frac{\Omega_\parallel}{\gamma} - w_x\frac{\Omega_\perp F}{4\gamma}\sinh(2k_0y)\,, \tag{10}$$

$$\dot{u}_{zs} = 0\,.$$

Thus $u_{zs} = \text{const}$. Evaluating the rapidly varying part of (3) yields

$$w_x = \frac{\Omega_\perp F}{\gamma k_0} \sim 0(\delta)\,,$$
$$w_y = \frac{\Omega_\parallel w_x}{\gamma k_0 u_{zs}} = -\frac{\Omega_\perp\Omega_\parallel}{\gamma^2 k_0^2 u_{zs}} \sim O(\delta^2)\,. \tag{11}$$

The ordering assumptions (9) are indeed satisfied, as can be seen from Eqs. (10) and (11).

The slow-scale equations (10) can be written in the vector form, i.e.,

$$\dot{\mathbf{u}}_s = \frac{\Omega_\parallel}{\gamma}\hat{e}_z \times \mathbf{u}_s + F_p\hat{e}_y\,, \tag{12}$$

where the effective slowly varying "force" F_p is given by

$$F_p = -\frac{\Omega_\perp^2 F^2}{4k_0\gamma}\sinh(2k_0y)\,. \tag{13}$$

Equation (13) represents a *ponderomotive*-type force, i.e., has its origin in the vector product between the rapidly oscillating off-axis z component of the wiggler field $[B_{wz} = -B_\perp F\sinh(k_0y)\sin(k_0z)]$ and the x component of the electron velocity $[u_{xf} = w_x\cosh(k_0y)\sin(k_0z)]$ averaged over the fast-time scale. One recognizes, of course, that Eq. (13) describes the usual focusing force in linear wigglers without the guide field. The general solution of (12) is

$$u_{ys} = u_0\cos\left(\frac{\Omega_\parallel}{\gamma}\tau + \phi_0\right)\,,$$
$$u_{xs} = u_0\sin\left(\frac{\Omega_\parallel}{\gamma}\tau + \phi_0\right) + u_d\,, \tag{14}$$

where the drift velocity in the x direction is given by

$$u_d = \frac{\Omega_\perp^2}{4k_0\gamma\Omega_\parallel}\sinh(2k_0y)\,, \tag{15}$$

and ϕ_0 is the initial phase. The first equation in (14) predicts *slow* betatron oscillations in the y direction, the amplitude of which can be negligible if the transverse velocity u_0 is sufficiently small. This transverse velocity depends on the beam emittance and entrance conditions into the wiggler. It will be shown below that reasonable values of u_0 are sufficiently small to justify our assumption of the approximate constancy of y in (7) and in expression (13) for the ponderomotive force. Figure 1 shows the numerical solution of Eqs. (3) in the case $\gamma = 9.6$, $\lambda_w = 2$ cm, $B_\parallel = 5$ kG, $B_\perp = 2$ kG, and $L = 10$ cm, subject to the following initial conditions (at $\tau = 0$): $x = 0$, $y = 0.2$ cm, $z = -15$ cm, $u_x = u_y = 0$, and $u_z = (1 - 1/\gamma^2)^{1/2}$. Fast oscillations with the wiggler period, slow betatron oscillations due to the guide field, and the drift in the x direction are seen in the figure. The drift motion of the off-axis electrons in a linear wiggler FEL with a guide field was first observed in calculations by Pasour *et al.*[6] In Ref. 6, the drift velocity was obtained from a fit to the numerical data and was found to have the same functional form as Eq. (15). The analytic theory developed above describes the beam transport in

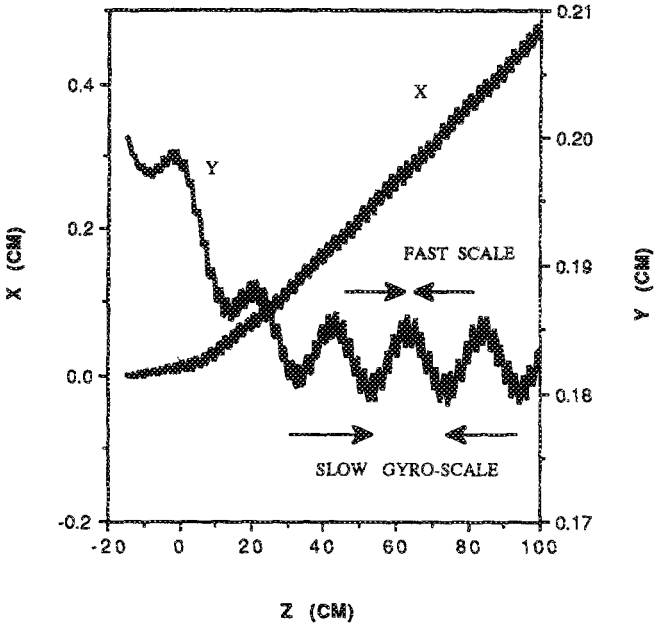

FIG. 1. A typical electron orbit in combined linear wiggler and axial guide magnetic fields. The parameters are $\gamma = 9.6$, $\lambda_w = 2$ cm, $B_\parallel = 5$ kG, $B_\perp = 2$ kG, $L = 10$ cm, and initially (at $z = -15$ cm $= 0$, $y = 0.2$ cm, $u_x = u_y = 0$).

combined linear wiggler and guide magnetic fields. We shall show in the next section how this theory can be modified to describe more complex magnetic field configurations which result in a complete radial confinement and stabilization of the beam.

III. ROTATIONAL TRANSFORMATION

In this section the possibility of a *slow* spatial variation of the ponderomotive force [see Eq. (13)] is considered. The previous analysis remains valid in this case with Eq. (12) replaced by

$$\dot{\mathbf{u}}_s = \frac{\Omega_\parallel}{\gamma}\,\hat{e}_z \times \mathbf{u}_s + \mathbf{F}_p(\tau)\,, \tag{16}$$

where $\mathbf{F}_p$ may vary slowly in amplitude, or direction, or both. Since a constant $\mathbf{F}_p$ in the y direction leads to the drift in the x direction, one can try to suppress the drift by introducing an *oscillating* ponderomotive force. This may be accomplished by adiabatically rotating the direction of polarization of the wiggler field along the wiggler axis, so that at a given z the *direction* of the wiggler field is along the vector

$$\hat{e}_{yr} = \hat{e}_x \sin(k_r z) + \hat{e}_y \cos(k_r z)\,, \tag{17}$$

where $k_r = 2\pi/\lambda_r$ and $\lambda_r (\lambda_r \gg \lambda_w)$ is the rotation pitch. The wiggler field in the laboratory frame will then be [see Eq. (1)]

$$\begin{aligned} B_x &= B_\perp \cos(k_0 z)\cosh(k_0 y_r)\sin(k_r z)\,, \\ B_y &= B_\perp \cos(k_0 z)\cosh(k_0 y_r)\cos(k_r z)\,, \end{aligned} \tag{18}$$

where

$$y_r = x \sin(k_r z) + y \cos(k_r z) \tag{19}$$

is the projection of the radius vector $\mathbf{r} = (x,y,z)$ in the direction of vector $\hat{e}_{yr}$. The slow-scale equation (16) for this case becomes

$$\dot{\mathbf{u}} = \frac{\Omega_\parallel}{\gamma}\,\hat{e}_z \times \mathbf{u}_s - f \sinh(2k_0 y_r)\,\hat{e}_{yr} \tag{20}$$

where

$$f = \frac{1}{k_0}\left(\frac{\Omega_\perp}{2\gamma}\right)^2 . \tag{21}$$

In order to analyze Eq. (20), we first write this equation in component form:

$$\begin{aligned} \dot{u}_{sx} &= -u_{sy}\frac{\Omega_\parallel}{\gamma} - f \sinh(2k_0 y_r)\sin(k_r z)\,, \\ \dot{u}_{sy} &= u_{sx}\frac{\Omega_\parallel}{\gamma} - f \sinh(2k_0 y_r)\cos(k_r z)\,. \end{aligned} \tag{22}$$

Here we can use [see Eq. (19)]

$$z = u_{sz}\tau$$

and

$$y_r = R \sin(k_r z + \beta) = R \sin(\omega\tau + \beta)\,, \tag{23}$$

where

$$R = (x^2 + y^2)^{1/2}\,, \quad \tan\beta = y/x\,, \quad \omega = k_r u_{zs} \approx k_r\,,$$

and $\tau = 0$ is associated with the axial position $z = 0$.

The ponderomotive force terms in (22) are now products of two correlated oscillating functions and thus, in principle, the drift cannot be averaged to zero. Nevertheless, we shall show below that the drift can be *reduced* by the rotation of the wiggler polarization. Under certain conditions the drift becomes purely *azimuthal*, thus resulting in the radial stability of the beam. Assuming the existence of a *slow azimuthal drift*, characterized by a linear velocity $\mathbf{u}_{ad}$ such that

$$\omega_D = |\mathbf{u}_{ad}|/R \ll \omega \approx k_r\,, \tag{24}$$

Eqs. (22) can be averaged over the "fast" rotation scale to yield

$$\begin{aligned} \langle \dot{u}_{sx} \rangle &= -\langle u_{sy} \rangle \frac{\Omega_\parallel}{\gamma} - k_0 f R \cos\beta\,, \\ \langle \dot{u}_{sy} \rangle &= \langle u_{sx} \rangle \frac{\Omega_\parallel}{\gamma} - k_0 f R \sin\beta\,. \end{aligned} \tag{25}$$

For simplicity, the analysis will be limited to small values of $k_0 y_r$ so that $\sinh(2k_0 y_r) \approx 2k_0 y_r$ in Eqs. (22). By writing

$$\beta = \omega_D \tau + \beta_0\,, \tag{26}$$

where β_0 is the initial phase, and by defining

$$\langle u \rangle = \langle u_{sx} \rangle + i\langle u_{sy} \rangle\,, \tag{27}$$

Eqs. (25) can be rewritten as

$$\langle \dot{u} \rangle = i\frac{\Omega_\parallel}{\gamma}\langle u \rangle - k_0 R f e^{i(\omega_D \tau + \beta_0)}\,. \tag{28}$$

This equation yields a rotating solution with constant radius R

$$\langle u\rangle = \langle u_0\rangle e^{i(\omega_D \tau + \beta_0)} . \tag{29}$$

where

$$\langle u_0\rangle = \frac{ik_0 f R}{\omega_D - (\Omega_\parallel/\gamma)} = \text{const} . \tag{30}$$

We then observe that

$$\omega_D = \frac{|\langle u_0\rangle|}{R}\,\text{sign}\left(\omega_D - \frac{\Omega_\parallel}{\gamma}\right) = \frac{k_0 f}{\omega_D - \Omega_\parallel/\gamma} . \tag{31}$$

The last equation yields two values for ω_D:

$$\omega_D^{\pm} = \frac{\Omega_\parallel}{\gamma} \pm \sqrt{\left(\frac{\Omega_\parallel}{\gamma}\right)^2 + \left(\frac{\Omega_\perp}{\gamma}\right)^2} . \tag{32}$$

One can see from Eq. (32) that the slowness condition, Eq. (24), is only satisfied when

$$(\Omega_\perp/\Omega_\parallel)^2 \ll 1 , \tag{33}$$

and the negative sign in Eq. (32) is used. In this case

$$\omega_D^- \approx -\Omega_\perp^2/4\gamma\Omega_\parallel . \tag{34}$$

The linear, azimuthal drift velocity associated with ω_D^- in Eq. (34) is given by

$$u_{ad} = |\omega_D^-|R = \frac{\Omega_\perp^2 R}{4\gamma\Omega_\parallel} , \tag{35}$$

which is equal to one half of the drift velocity in the nonrotating wiggler case [see Eq. (15)].

Figure 2(a) shows the results of a numerical solution of the exact momentum equations with the same parameters used in Fig. 1, but with the addition of a rotation with $k_r = 0.15\ \text{cm}^{-1}$ and an initial transverse velocity $\mathbf{u}_\perp = 0.006\,\hat{e}_y$, representing finite-beam emittance. The figure clearly demonstrates the predicted stabilizing role of the rotational transform. Furthermore, we observe that the azimuthal drift does not alter the form of the cross section of the beam if this cross section is initially circular. In this case the self-fields of the beam can be easily modeled for a uniform density N_e,

$$|\mathbf{E}| = 2\pi e N_e r , \quad |\mathbf{B}| = 2\pi e N_e r u_{zs} , \tag{36}$$

where $r \leqslant r_{\text{beam}}$ is the radial position in the beam and r_{beam} is the beam radius. The self-fields (36) have been included in calculations shown in Fig. 2(a) with the total beam current $I = 600$ A and $r_{\text{beam}} = 0.2$ cm. It may be noted that the case shown in the figure corresponds to $r \approx 0.2$, so that $2k_0 r = 1.25$ and therefore the small parameter expansion $\sinh(2k_0 y) \approx 2k_0 y$, used in deriving Eq. (34), is violated. Nevertheless, the azimuthal drift and the resulting radial stabilization are still apparent. Finally, the averaging technique is tested in Fig. 2(b) which shows the solution of the slow-scale equations (22) for the same parameters as Fig. 2(a). Comparing the two calculations we see that the slow-scale equations correctly describe the slow evolution of the trajectory and thus can be used in studying the beam transport. This allows us to avoid the numerical difficulties associated with resolving the fast scale in the exact momentum equations when studying the beam behavior for long times.

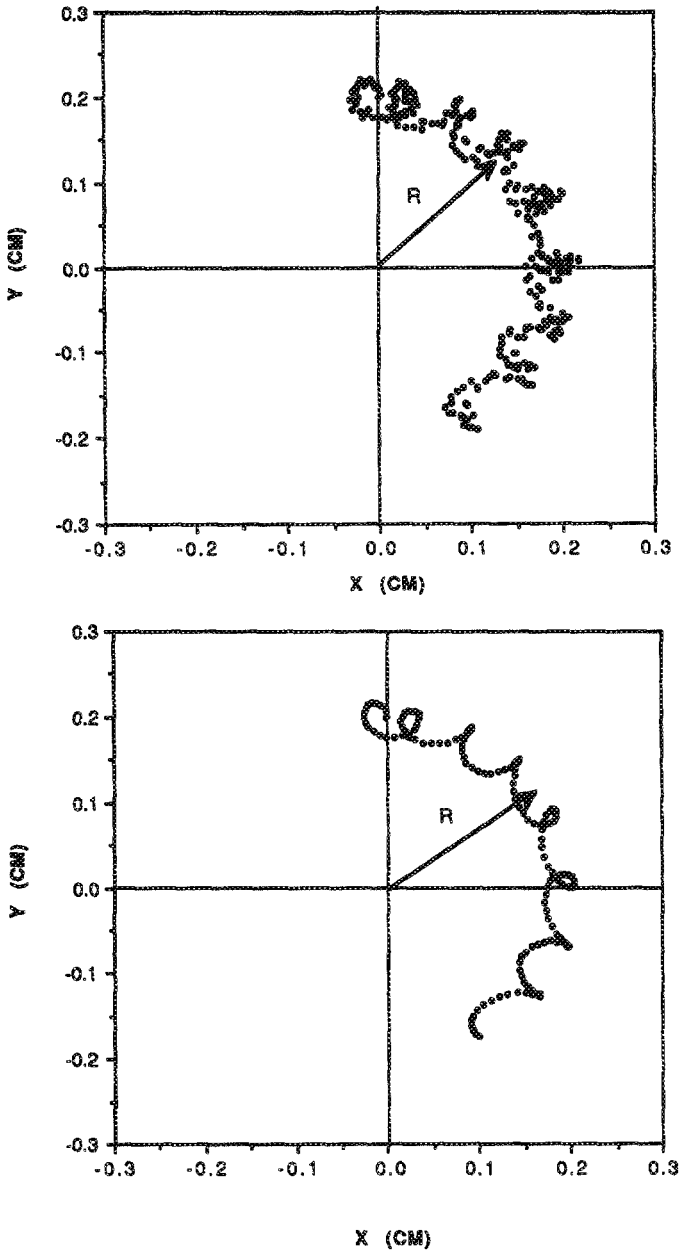

FIG. 2. (a) The mapping of the electron trajectory in the x-y plane in the rotating wiggler configuration with a guide field. The parameters are $\gamma = 9.6$, $\lambda_w = 2$ cm, $B_\parallel = 5$ kG, $B_\perp = 2$ kG, $L = 10$ cm (same as Fig. 1), $k_r = 0.15\ \text{cm}^{-1}$, $I = 600$ A, $r_b = 0.2$ cm, and initially (at $z = -15$ cm) $= 0$, $y = 0.2$ cm, and $u_x = 0$, $u_y = 0.006$. The mapping is shown for $\tau = 135$ cm and $\Delta\tau = 1.0$ cm. (b) the same mapping obtained using the long-scale, averaged equations. The parameters are as in (a).

In order to compare the results of the numerical calculations with the predictions of Eq. (35), slow-scale calculations were performed with the same parameters as Fig. 2(b), but with $B_\parallel = 10$ kG and the initial values $x = 0.1$ cm and $y = 0$. A much longer integration time of $\tau = 500$ cm corresponding to a longer wiggler length was used. The results of these calculations are shown in Fig. 3. The dots in the figure represent the mapping of the transverse electron position along the wiggler with the step size $\Delta\tau = 2$

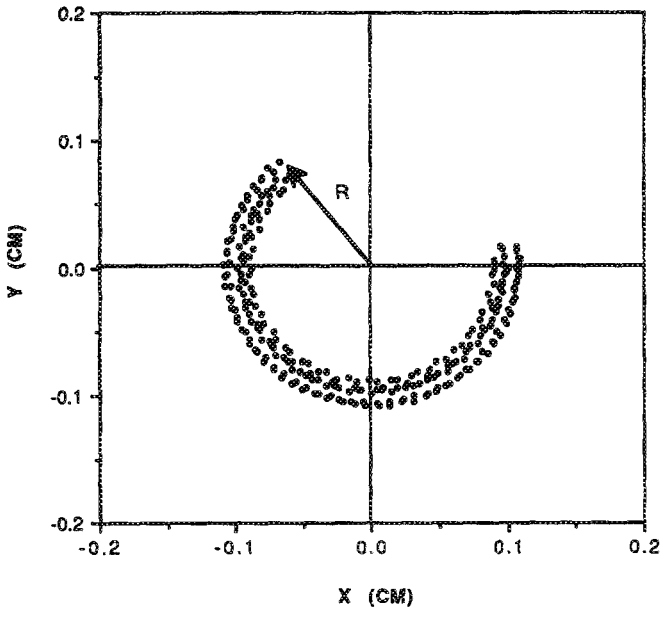

FIG. 3. Simulation of rotationally stabilized electron trajectory showing a high degree of radial confinement. The parameters are $\gamma = 9.6$, $\lambda_w = 2$ cm, $B_\parallel = 10$ kG, $B_\perp = 2$ kG, $L = 10$ cm, $k_r = 0.15$ cm^{-1}, $I = 100$ A, $r_b = 0.1$ cm, and initially (at $z = -15$ cm) $x = 0.1$, $y = 0$, $u_x = 0.006$, $u_y = 0$. The simulation time is $\tau = 500$ cm and $\Delta\tau = 2$ cm.

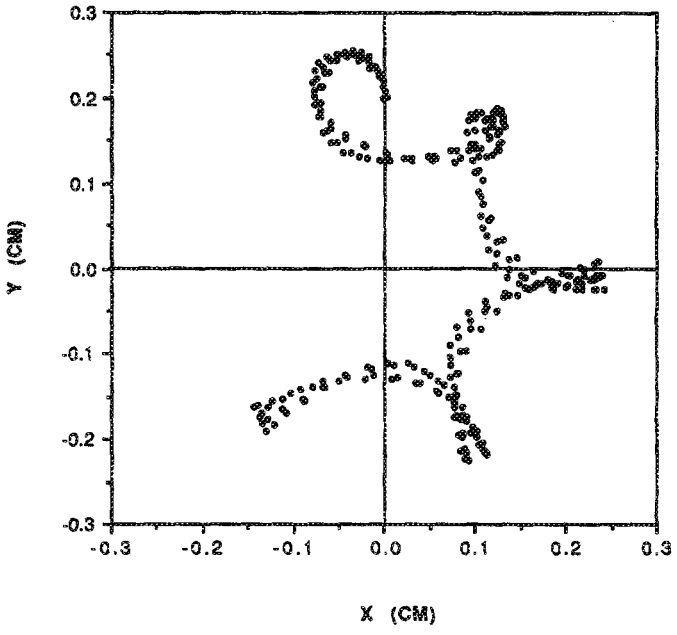

FIG. 4. Trajectory mapping in the x-y plane for the same parameters as in Fig. 2(a) except $B_\parallel = B_\perp = 2$ kG and $I = 0$.

cm. A high degree of radial beam stability can be seen in the figure. Also, in the case considered, $\omega_D^- \approx 0.00625$ cm^{-1} so that the azimuthal drift angle during the integration time ($\tau = 500$ cm) should be $\Delta\beta = \omega_D^- \tau \approx \pi$. The 30% larger angle $\Delta\beta \approx 1.3\pi$ obtained in the calculations can be explained by the azimuthal drift with the velocity $E_{\rm self}/\gamma^2\beta_\parallel$ due to the self-fields of the beam.

We now discuss the conditions necessary for stable beam operation in the rotating wiggler configuration. The radial stabilization is destroyed if any of the assumptions which led to the azimuthal drift theory are violated. For example, Fig. 4 shows a case with the same parameters as Fig. 2(a) (exact momentum equations), but with $I = 0$ and $k_r = 0.018$ cm^{-1} so that the rotation is too slow, i.e., $\omega_D^- \sim k_r$ in violation of (24). These conditions result in a gradual but steady *increase* in the radical position of the test electron. Another example of poor stability is shown in Fig. 5, in which the same parameters as Fig. 2(a) are again used except $I = 0$ and $B_\parallel = B_\perp (= 2$ kG) in violation of condition (33). In this case the drift is too fast and the circular motion is only a very rough approximation of the actual trajectory shown in Fig. 5. Finally, the condition that determines which of the two solutions ω_D^+ and ω_D^- is valid was investigated. We found that the solution is determined by the direction of the rotation of the wiggler polarization relative to the cyclotron motion in the guide field. The situation of rotation in the wrong direction is shown in Fig. 6. The parameters are again as in Fig. 2(a), but $I = 0$ and $k_r = -0.15$ cm, so that the wiggler polarization vector rotates in the direction of the electron gyration in the guide field. The figure shows that a very rapid azimuthal electron motion results. The motion is characterized by the fast frequency, $\omega_D^+ \approx \Omega_\parallel/\gamma$, is radially unstable, and thus inappropriate for FEL applications.

Finally, we shall address the important issue of the FEL radiation coupling to the rotating electron beam. The wiggle velocity in the rotating beam is always perpendicular to the direction of the polarization of the wiggler field. Therefore, the polarization of the wiggle velocity rotates slowly with distance along the axis. This rotation may, in principle, destroy the FEL gain for a conventional, linearly

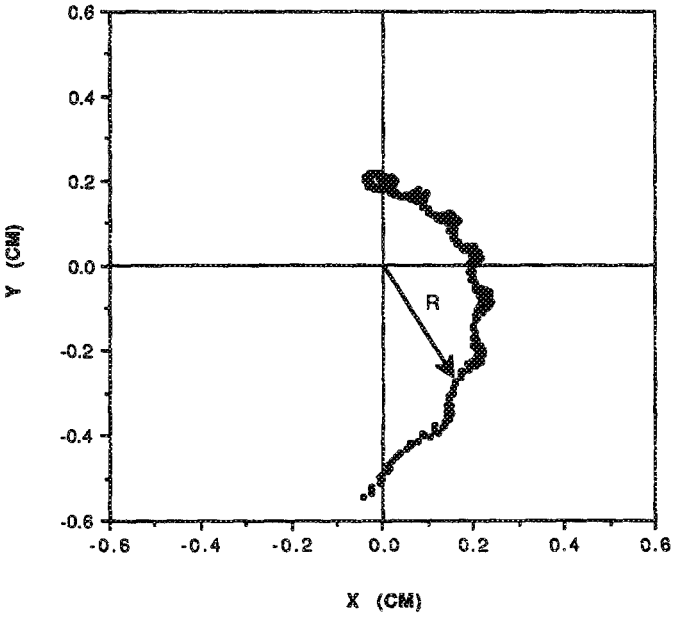

FIG. 5. Trajectory mapping in the x-y plane for the same parameters as in Fig. 2(a), except $I = 0$ and $k_r = 0.018$ cm^{-1} (the wiggler rotation is too slow).

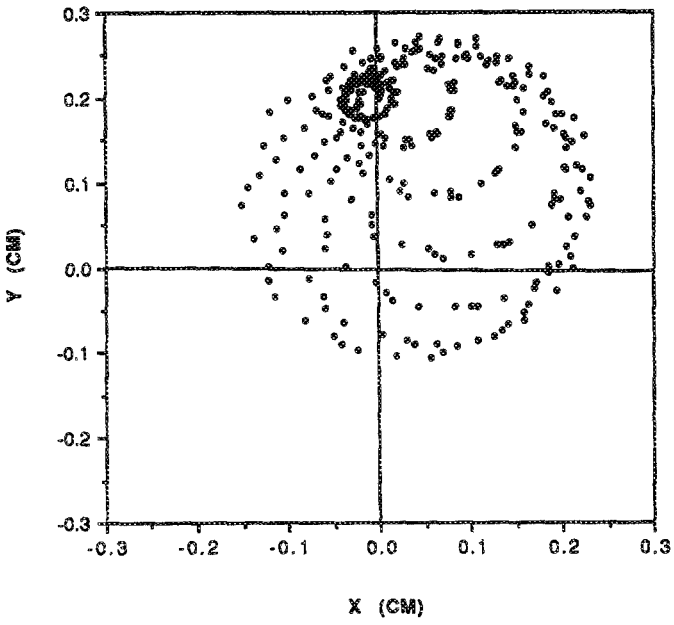

FIG. 6. Trajectory mapping the x-y plane showing poor beam stability for the case of the wiggler polarization direction rotating in the same direction as the electron gyromotion. The parameters are the same as in Fig. 2, except $I=0$ and $k_r=-0.15\ \mathrm{cm}^{-1}$.

polarized, electromagnetic wave. The problem can be resolved if one gradually rotates the wave polarization so that it always remains perpendicular to the direction of the wiggler field and thus parallel to the wiggle velocity in the beam. For example, in a rectangular cross-section waveguide FEL configuration the required rotation of the polarization can be achieved by a slow twisting of the waveguide along the axis with a pitch of $2\pi/k_r$. If this polarization rotation is sufficiently slow, then one can expect that all the results of the conventional linear wiggler FEL theory should be applicable to the rotating beam FEL.

IV. CONCLUSIONS

(i) Off-axis electrons in combined linear wiggler and guide magnetic fields drift transversely to the direction of the wiggler field, thus destroying the radial localization of the beam.

(ii) The origin of the transverse motion lies in the $\mathbf{F}\times\mathbf{B}$ drift in the guide field due to a ponderomotive-type force which is the result of the product of the rapidly oscillating transverse electron velocity and the off-axis axial component of the wiggler field averaged over the wiggler period. An expression for the drift velocity is obtained by averaging equations of motion over the wiggler wavelength scale.

(iii) Rotation of the wiggler polarization direction around the axis results in a slow azimuthal drift with a magnitude equal to one half the drift velocity without the rotation. Radial confinement of the beam is obtained for rotation wave numbers which are much smaller than the wiggler wave number provided certain conditions are satisfied.

(iv) The theory shows that radial confinement and stabilization are achieved when (a) $(B_\perp/B_\parallel)^2 \ll 1$, (b) the wiggler rotation speed is much faster than the drift velocity, and (c) the wiggler polarization vector rotates in the direction opposite to the gyromotion of the electrons in the guide field.

(v) The theory was tested in numerical simulations which included the effects of beam self-fields and finite beam emittance. These calculations showed that radial stabilization can be achieved in the presence of these real beam effects.

ACKNOWLEDGMENT

This work was supported by the U. S. Department of Energy under contract No. DEAC01-88ER80582.

[1] K. Halbach, Nucl. Instrum. Methods **187**, 109 (1981).
[2] C. W. Roberson and P. Sprangle, Phys. Fluids B **1**, 3 (1989), and references therein.
[3] T. J. Orzechowski, B. R. Anderson, W. M. Fawley, D. Prosnitz, E. T. Scharlemann, S. M. Yarema, A. M. Sessler, D. B. Hopkins, A. C. Paul, and J. S. Wurtele, Nucl. Instrum. Methods Phys. Res. A **250**, 144 (1986).
[4] E. T. Scharlemann, J. Appl. Phys. **58**, 2154 (1985).
[5] K. E. Robinson, D. C. Quimby, J. M. Slater, T. L. Churchill, A. Pindroh, and A. Valla, Nucl. Instrum. Methods Phys. Res. A **250**, 100 (1986).
[6] J. A. Pasour, C. W. Roberson, and F. Mako, J. Appl. Phys. **53**, 7174 (1982).